Figure S1

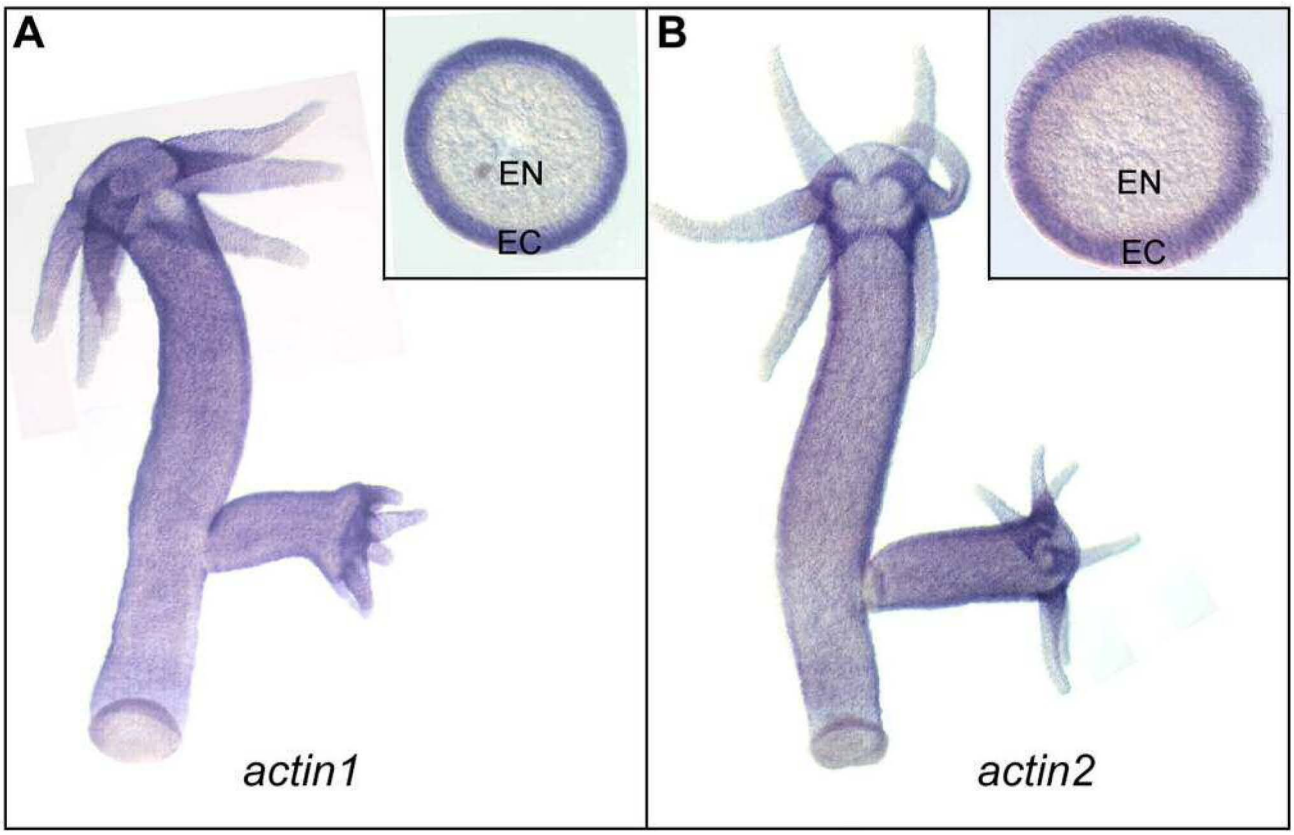

Fig. S1. Spatial expression patterns of the *Hydra actin1* and *actin2* genes (XP_002154462, XP_002154696). **(A,B)** Uniform distribution of *actin1* and *actin2* mRNAs throughout the entire body column as revealed by whole mount in situ hybridization. Inserts show a cross section through the gastric region revealing that both genes are expressed at a significantly higher level in the ectoderm (EC) than in the endoderm (EN).

Figure S2

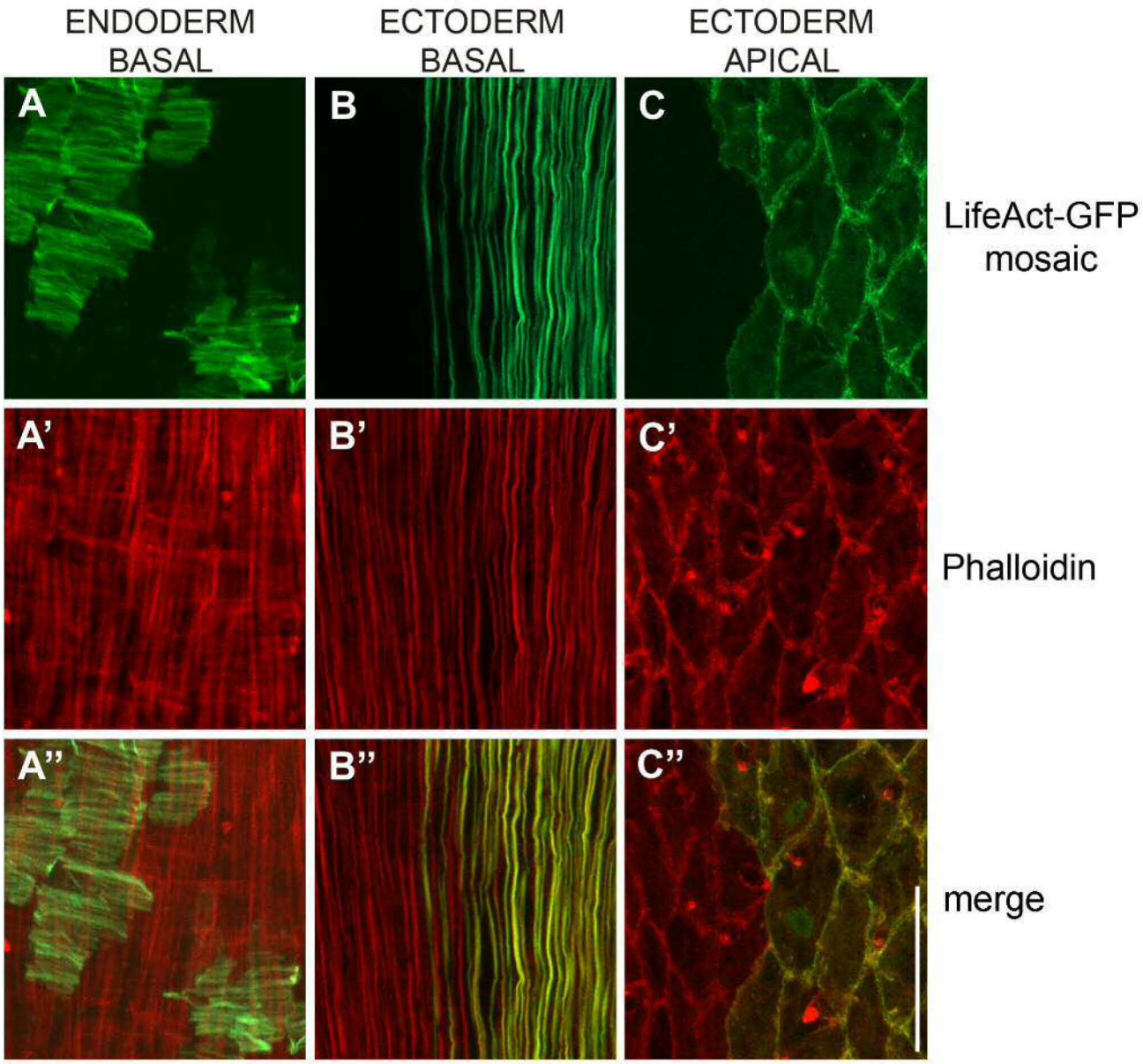

Fig. S2. Localization of Lifeact-GFP and Phalloidin to the same F-actin structures in *Hydra* epithelial cells. **(A-C)** Double detection in mosaic transgenic Lifeact-GFP tissue fixed and stained with rhodamine-labelled Phalloidin shows that both methods used to visualize F-actin result in total overlap of the signal. **(A-A")** Confocal projection (11 µm depth) at the level of muscle processes in an endodermal transgenic polyp. **(B-B")** Confocal projection (12 µm depth) at the level of muscle processes in an ectodermal transgenic polyp. **(C-C")** Confocal projection (3.5 µm depth) at the level of apical cell junctions in the same cells as in **(B-B")**. Scale bar: 50 µm.

Figure S3

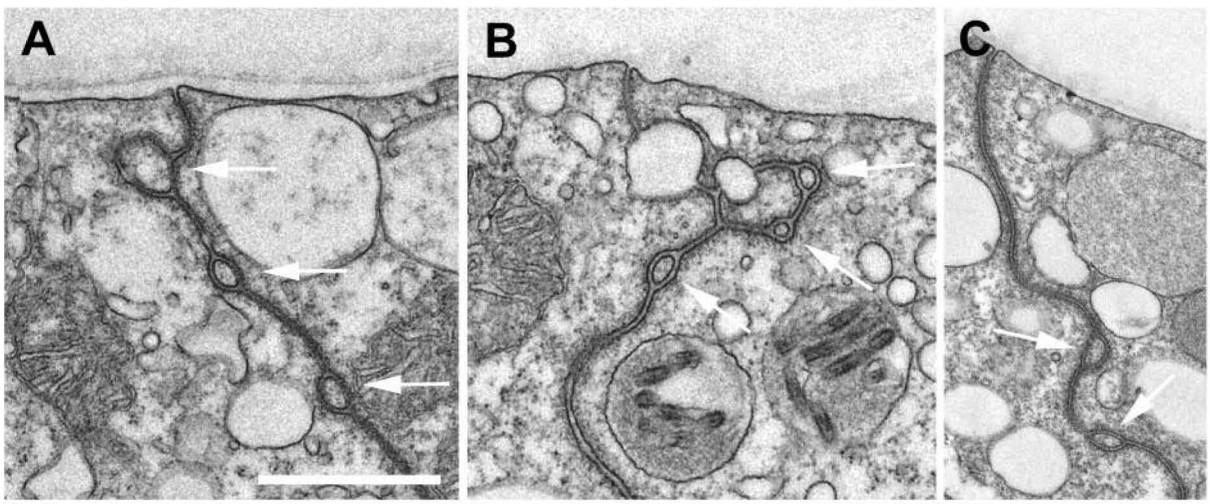

Fig. S3. Ultrastructural localization of filopodia-like protrusions at apical septate junctions. **(A-C)** Representative examples of cytoplasmic fingers (arrows) located between two ectodermal epithelial cells and connected with both cells by septate junctions. These protrusions can be frequently seen in the most apical-lateral areas of epithelial cells. For ultrastructural analysis, *Hydra* polyps were subjected to conventional transmission electron microscopy by using chemical fixation and standard techniques. Scale bar for **(A-C)**: 1 µm.

Figure S4

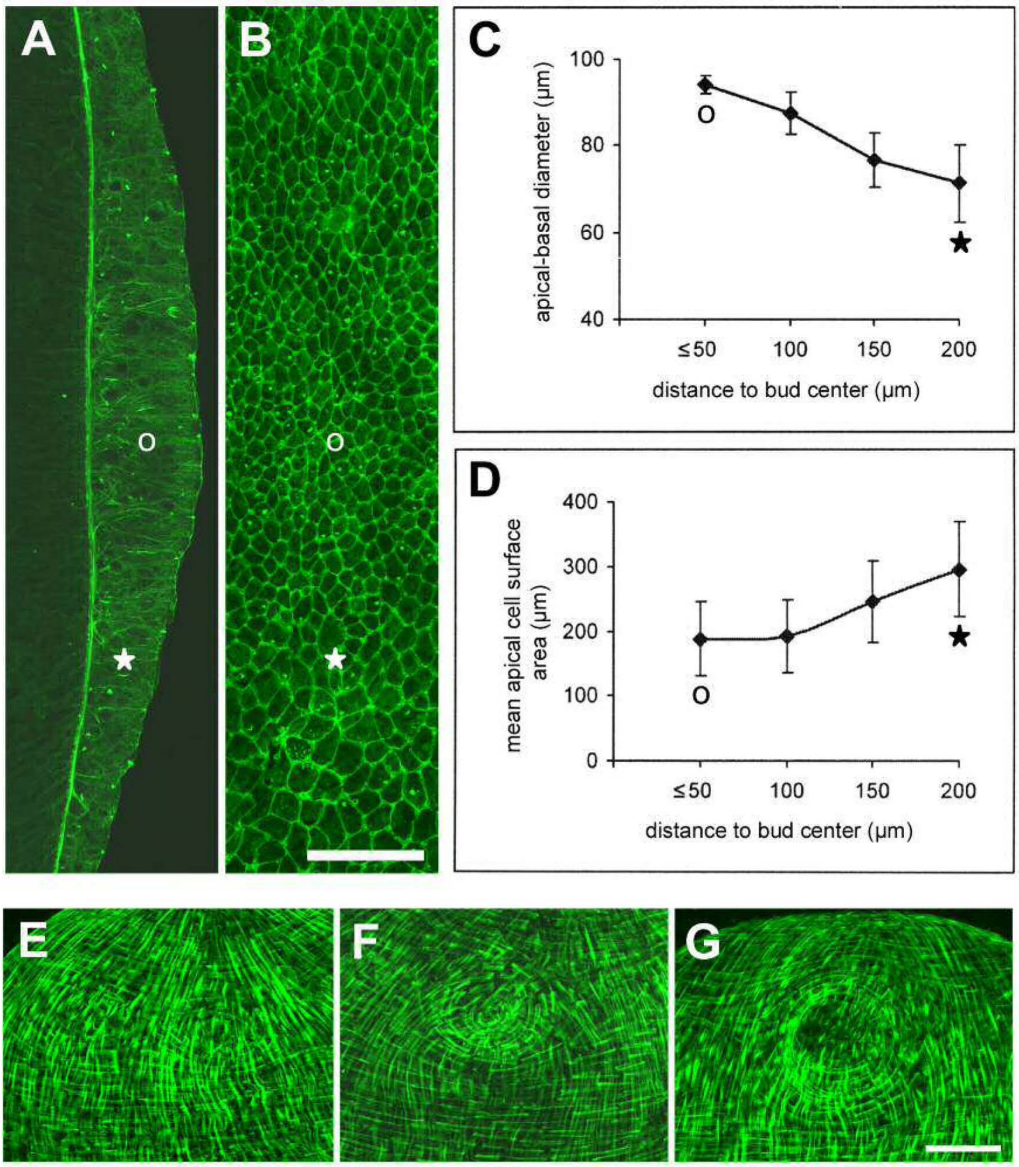

Fig. S4. Cell shape changes during epithelial thickening in the bud anlage and circular arrangement of endodermal myonemes during tentacle formation. **(A,B)** Confocal projections of a stage 1 bud fixed and stained with Alexa Fluor 488-Phalloidin. **(A)** A lateral view shows that epithelial cells in the center of the thickened area have clearly enlarged their apical-basal diameter, while their planar diameter at the apical surface as shown in **(B)** has significantly decreased. **(C,D)** Measurements of apical-basal diameters **(C)** and apical cell surface areas **(D)** of ectodermal epithelial cells at different distance to the center of the thickened area. Each data point represents mean±S.D. of at least 20 cells. Circles label the center of the thickened area; stars define peripheral regions at a distance of about 200 µm. **(E-G)** Confocal projections of basal regions of ectodermal and endodermal epithelial cells in the head part of late budding stages stained with Alexa Fluor 488-Phalloidin. **(E)** Eye-shaped arrangement of endodermal muscle processes just prior to evagination of tentacles. **(F)** Circular arrangement of endodermal muscle processes at the onset of tentacle evagination. **(G)** Circular arrangement of endodermal muscle processes, when small tentacle protrusions are visible. Scale bars: **(A,B)** 100 µm; **(E-G)** 50 µm.

Figure S5

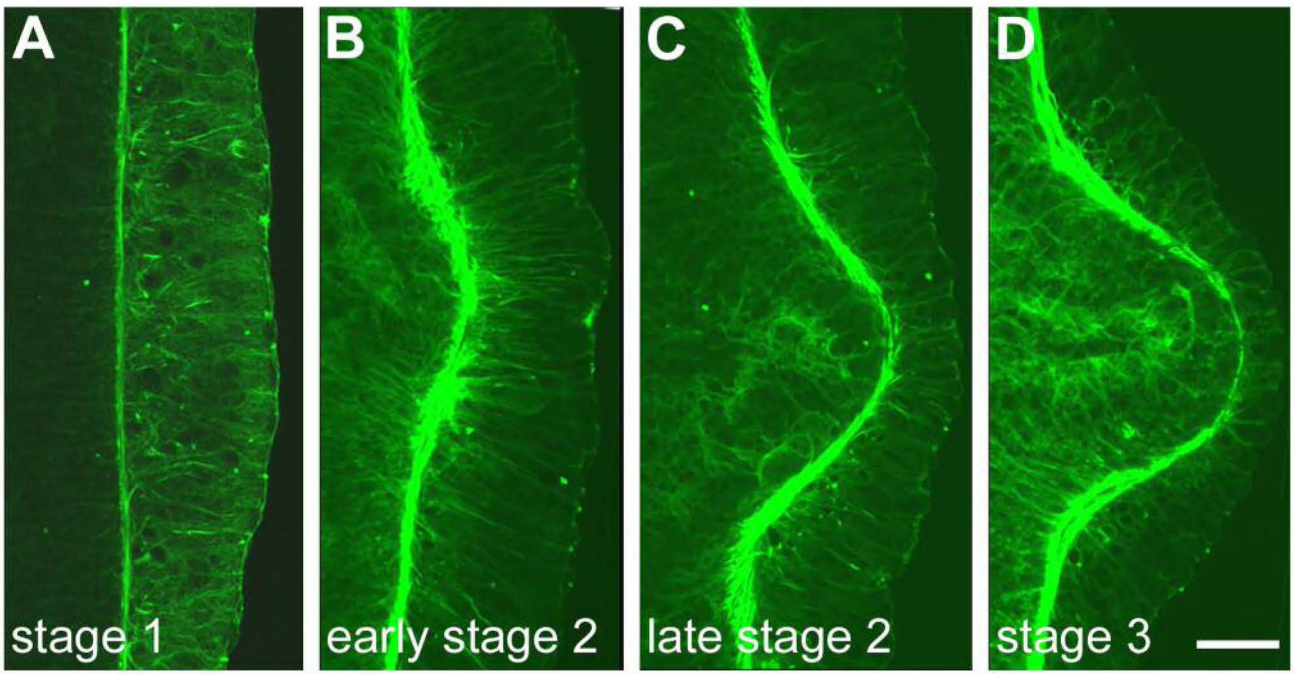

Fig. S5. Confocal projections of lateral views on the evaginating tissue bilayer. (**A**) Ectodermal thickening in the budding region at bud stage 1. (**B**,**C**) Bending of the endodermal into the ectodermal tissue layer at bud stage 2 associated with a shortening of the apicobasal dimension in ectodermal epithelial cells. (**D**) Evagination of the tissue bilayer at bud stage 3. All samples were stained with Alexa Fluor 488 Phalloidin. Scale bar: 100 m.

Figure S6

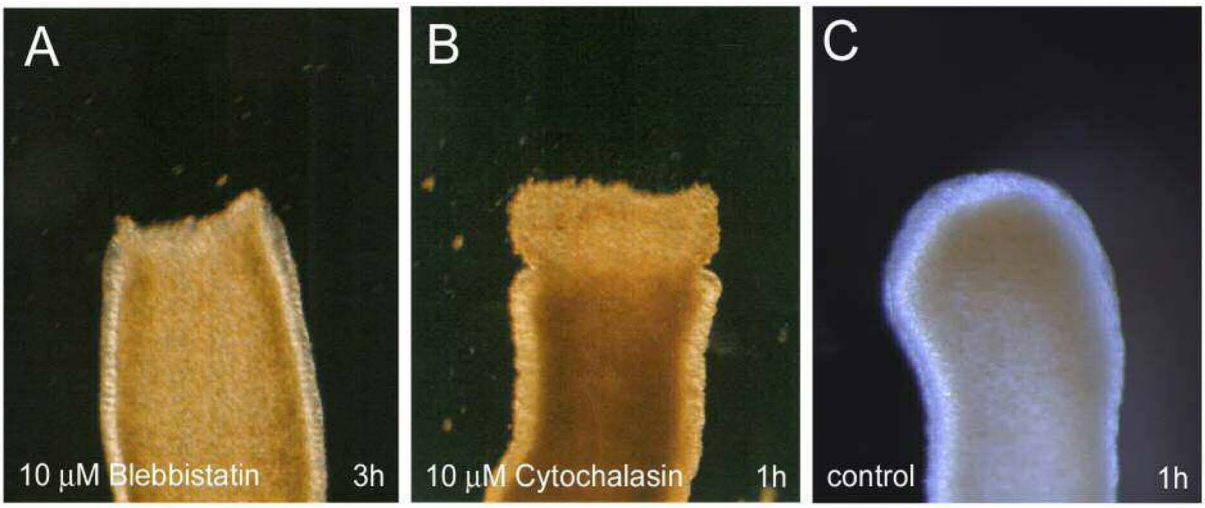

Fig. S6. Effects of actin and myosin inhibitors on head regeneration.
(**A,B**) Blebbistatin (inhibitor of myosin light chain kinase) and CytochalasinD (inhibitor of actin polymerization) block wound healing. Head regenerates were incubated immediately after decapitation in 10 µM Blebbistatin (Sigma) in 0.1 %DMSO or 10 µM CytocalasinD (Alexis Biochemicals) in 0.1 % Methanol and kept in inhibitor solution throughout the regeneration process. (**A**) Blebbistatin-treated regenerates failed to close their wound without showing tissue disintegration. Treated regenerates lost contractile behaviour in the entire polyp. Hence, actomyosin contractility seems to be required for wound healing. (**B**) CytochalasinD-treated head regenerates failed to close their wound. The endodermal epithelial layer separated from the ectoderm and leaked from the site of cutting. The endoderm has been shown to be the first tissue to seal the wound by remodeling cell shapes and cell polarities. Disassembly and polymerization of actin fibers may be critically involved in these processes.
(**C**) Untreated DMSO control regenerate.

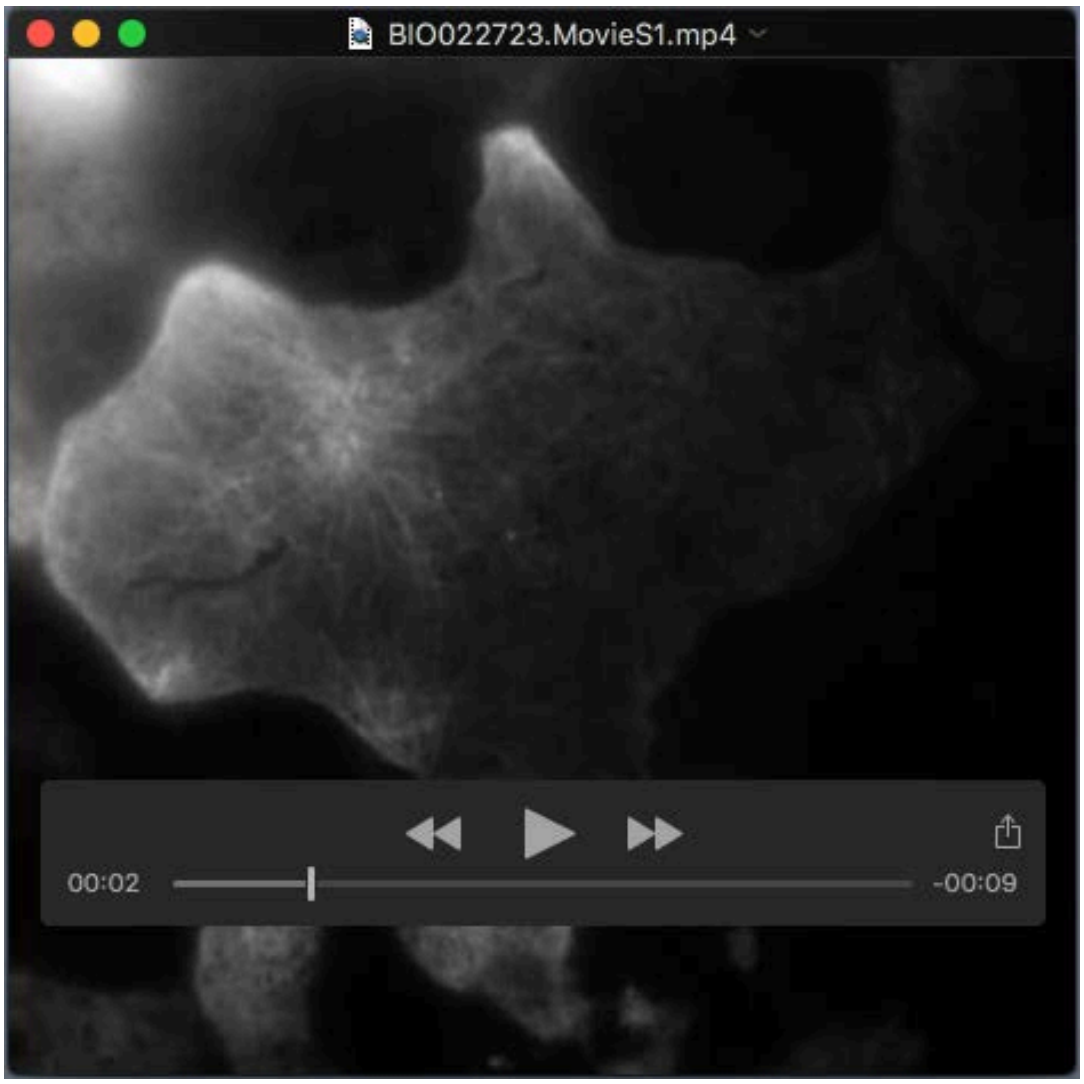

Movie 1. Actin dynamics in apical cortical networks. TIRF microscopy movie showing cortical actin dynamics just below the apical cell membrane in a Lifeact-GFP-positive ectodermal epithelial cell over a period of 222 seconds.

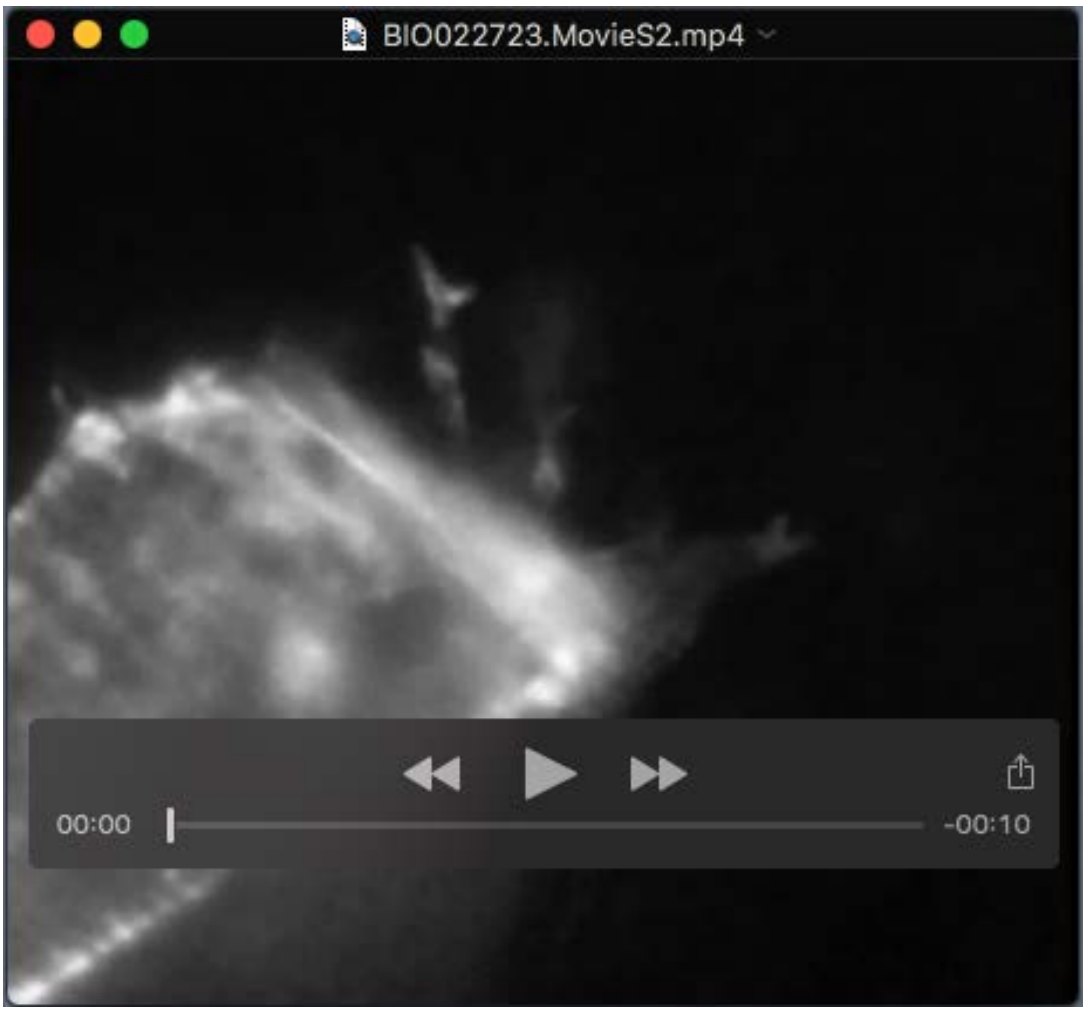

Movie 2. Actin dynamics in apical filopodia-like protrusions. TIRF microscopy movie showing the apical junctional region in a Lifeact-GFP-positive ectodermal epithelial cell over a period of 138 seconds. The black area around the transgenic cell is occupied by non-transgenic ectodermal epithelial cells.

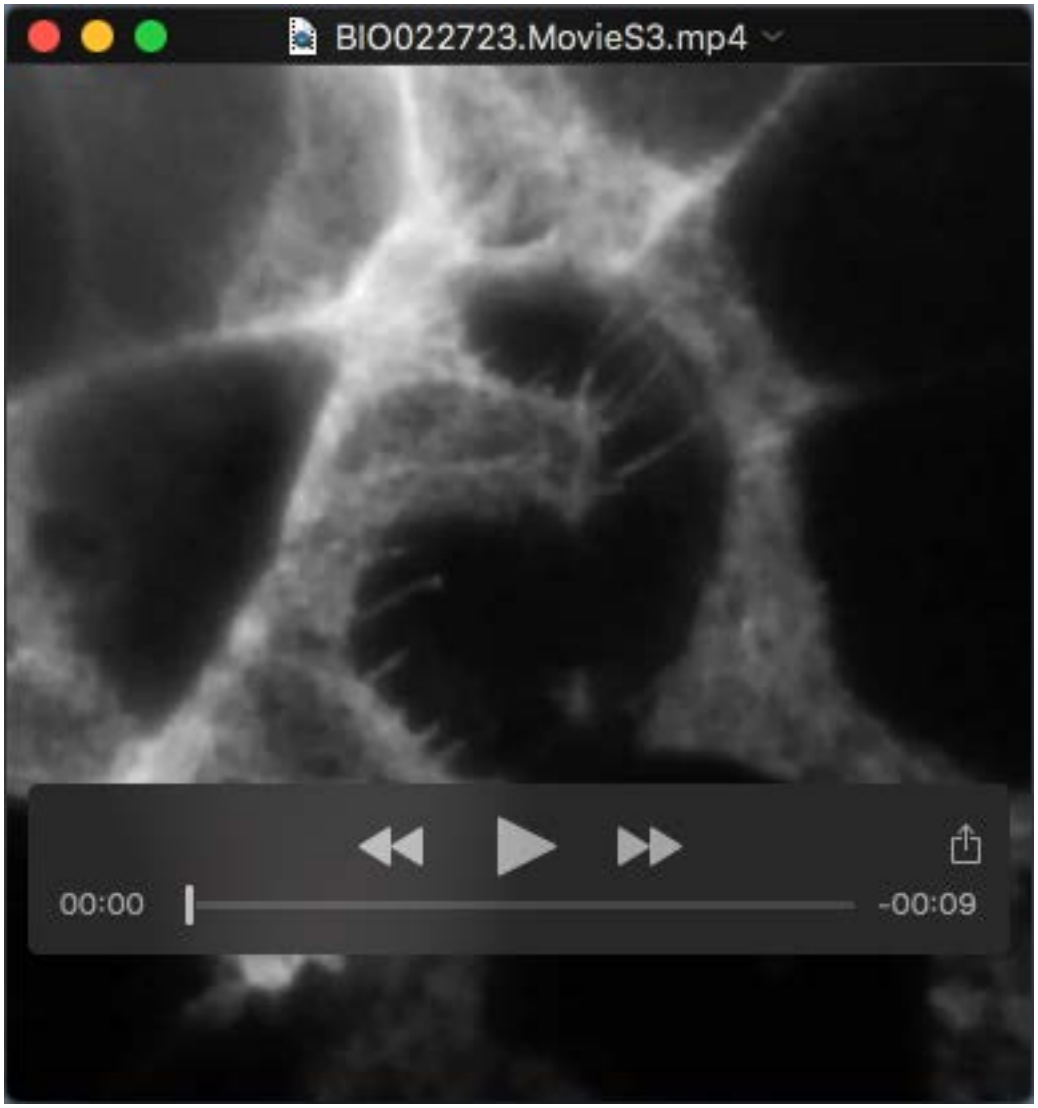

Movie 3. Detachment of apical filopodia. TIRF microscopy movie showing detachment of two Lifeact-GFP-positive ectodermal epithelial cells across a non-transgenic cell over a period of 132 seconds.